

Comparing of optical properties and morphology of polyoxadiazoles with CF_3 groups

B. Hajduk ^{a,b,*}, **P. Jarka** ^a, **J. Weszka** ^{a,b}, **M. Bruma** ^c, **J. Jurusik** ^b,
M. Chwastek ^{a,b}, **D. Mańkowski** ^a

^a Division of Materials Processing Technology, Management and Computer Techniques in Materials Science, Institute of Engineering Materials and Biomaterials, Silesian University of Technology, ul. Konarskiego 18a, 44-100 Gliwice, Poland

^b Department of Physics, Center of Polymer and Carbon Materials, Polish Academy of Sciences, ul. M. Curie-Skłodowska 34, 41-819 Zabrze, Poland

^c Institute of Macromolecular Chemistry, Aleea Gr. Ghica Voda 41A, Iasi, Romania

* Corresponding author: E-mail address: bhajduk@cchp-pan.zabrze.pl

Received 16.02.2010; published in revised form 01.05.2010

Materials

ABSTRACT

Purpose: The aim of this paper is to compare optical properties of 4-(1,1,1,3,3,3-hexafluoro-2-(4-(3(4-(5-(4-m-tolyoxy)phenyl)-1,3,4-oxadiazol-2-yl)phenoxy)phenylcarbonyl)phenyl)propan-2-yl)-N-methylbenzamide (Oxad 6F-D) and 4-(1,1,1,3,3,3-hexafluoro-2-(4-(4-(5-(4-(p-tolyoxy)phenyl)-1,3,4-oxadiazol-2-yl)phenoxy)phenyl)propan-2-yl)-N-methylbenzamide (Oxad 6F-E).

Design/methodology/approach: The Oxad 6F polymer thin films were deposited onto glass and KBr substrates by spin-coating method under different technological conditions.

Findings: The spinning rate V and solution concentration C influenced optical properties of Oxad 6F-D and Oxad 6F-E thin films. The goal of this paper is to show differences in properties of these polymers.

Research limitations/implications: The electrical and luminescent properties of Oxad 6F polymers will be carried out in the nearest time. The different properties of these polymers are caused by benzene position in the polymer chain, two aromatic rings are in meta-position in Oxad 6F-D and all benzene rings are in para-positions in Oxad 6F-E.

Practical implications: Thin films of Oxad 6F-D and Oxad 6F-E are good potential material for applications in polymer optoelectronic devices.

Originality/value: The aim of this paper is to describe the optical properties of Oxad 6F polymers prepared under different technological conditions.

Keywords: UV-Vis spectroscopy; AFM microscopy; IR spectroscopy; Spin-coating method; Organic polymer

Reference to this paper should be given in the following way:

B. Hajduk, P. Jarka, J. Weszka, M. Bruma, J. Jurusik, M. Chwastek, D. Mańkowski, Comparing of optical properties and morphology of polyoxadiazoles with CF_3 groups, Journal of Achievements in Materials and Manufacturing Engineering 40/1 (2010) 7-14.

1. Introduction

Polyoxadiazoles [1-5] are polymers having in the backbone oxadiazol group, five member ring consisting of two nitrogen, two carbon and oxygen atoms. In the oxadiazol group each nitrogen atom is linked with carbon atom by a double bond. Some of polyoxadiazoles can be used as a base for nanocomposites [6].

Oxad-6F-D and Oxad-6F-E are polyoxadiazoles containing six fluorine atoms [7-8] linked by single bonds to carbon atoms between two phenylene rings along with the polymer chain.

Most frequently used methods for polymer thin films deposition are the chemical vapour deposition (CVD) [9-12], also known as chemical transport in vapour phase, and the spin-coating method [13-15].

Chemical vapor methods used to prepare thin films of polyzomethines are based on transporting monomers in vapor phase by transport agent towards the substrate, where polymer thin film is grown by polycondensation process.

The spin coating method is based on spinning the substrate with some quantity of polymer solution put onto it.

2. Experimental

Two fluorine-containing polyoxadiazoles have been studied: (Fig. 1)

4-(1,1,1,3,3,3-hexafluoro-2-(4-(3(4-(5-(4-m-tolyoxy)-phenyl)-1,3,4-oxadiazol-2-yl)phenoxy)phenylcarbonyl)phenyl)propan-2-yl)-N-methylbenzamide (Oxad 6F-D) and (Fig. 2) 4-(1,1,1,3,3,3-hexafluoro-2-(4-(4-(5-(4-(p-tolyoxy)phenyl)-1,3,4-oxadiazol-2-yl)phenoxy)phenyl)propan-2-yl)-N-methylbenzamide (Oxad 6F-E).

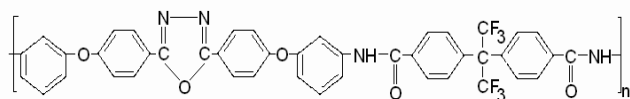


Fig. 1. Scheme of Oxad-6F-D polymer

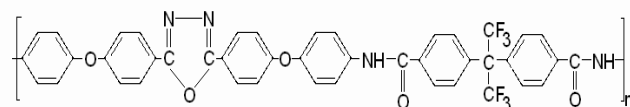


Fig. 2. Scheme of Oxad-6F-E polymer

Both polymers, Oxad-6F-D and Oxad-6F-E, were synthesized in the Institute of Macromolecular Chemistry, in Romanian Academy Sciences in Iasi. Tetrahydrofuran (THF) used as a solvent was purchased in POCH.

Two sets of THF solutions of polyoxadiazoles Oxad-6F-D and Oxad-6F-E were prepared, each one with three different concentrations. Polyoxadiazole films were spin-coated onto glass substrates and KBr pastilles.

In each series thin films were spin-coated with three different spinning rates V : 3000, 4000 and 5000 rpm. Technological parameters are shown in Table 1.

Table 1.
Technological parameters of spin-coating process

Oxad-6F-D			Oxad-6F-E		
C[%]	V [rpm]	t [s]	C[%]	V [rpm]	t [s]
0.8	3000	15	0.8	3000	15
	4000			4000	
	5000			5000	
1.7	3000	15	1.4	3000	15
	4000			4000	
	5000			5000	
2.1	3000	15	2.1	3000	15
	4000			4000	
	5000			5000	

UV-Vis absorbance spectra were taken on the as-prepared thin films with Ocean-Optics HR4000 spectrophotometer within 200-1000 nm wavelength range.

The topographic and sensor images were performed with Atomic Forces Microscope (AFM) and IR absorption spectra were recorded with IR spectrophotometer Specord M80 within 200-4000 cm^{-1} range. All the measurements were performed at room temperature.

3. Results

3.1. AFM measurements

Topographic and sensor images taken in contact mode on as-prepared thin films with Atomic Force Microscope are seen in Figs 3-8.

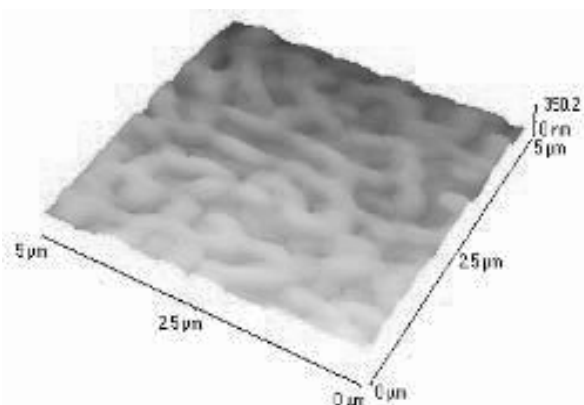


Fig. 3. AFM topographic image of Oxad-6F-D polymer film prepared from 1.7% THF-polymer solution, deposited with spinning rate $V=5000$ rpm

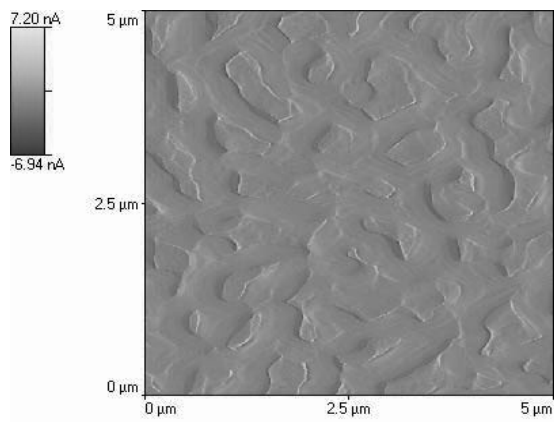


Fig. 4. AFM image of Oxad-6F-D polymer film deposited with 1.7% solution with spinning rate $V=5000$ rpm

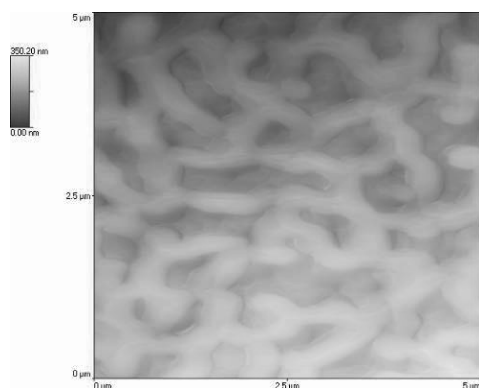


Fig. 5. AFM sensor image of Oxad-6F-D polymer film prepared with 1.7% solution with spinning rate $V=5000$ rpm

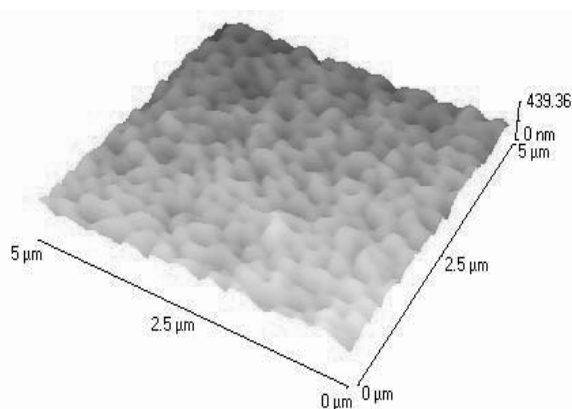


Fig. 6. AFM topographic image of Oxad-6F-E polymer film prepared from 1.4% THF-polymer solution, deposited with spinning rate $V=5000$ rpm

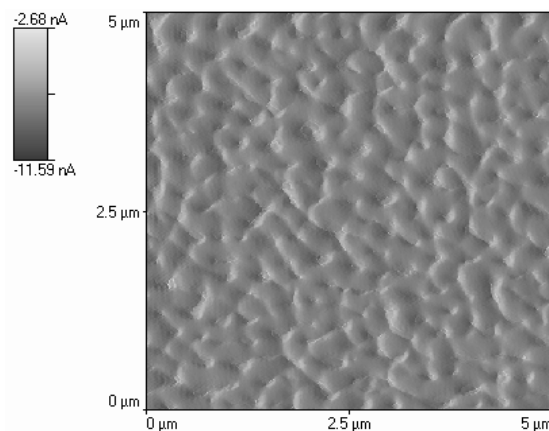


Fig. 7. AFM topographic image of Oxad-6F-E polymer film prepared from 1.4% THF-polymer solution, deposited with spinning rate $V=5000$ rpm

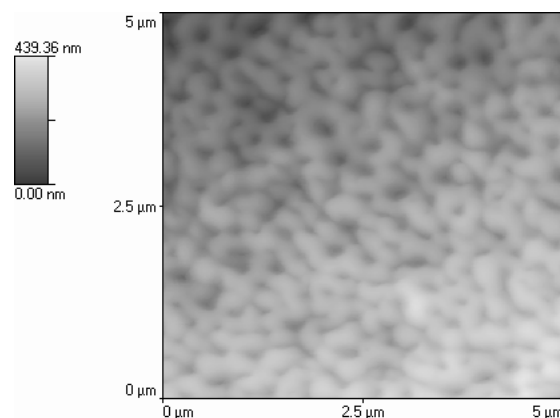


Fig. 8. AFM image of Oxad-6F-E polymer film prepared from 1.4% THF-polymer solution, deposited with spinning rate $V=5000$ rpm

The images of Oxad-6F-D and Oxad-6F-E thin films reveal granular morphology of surface. Surface of Oxad-6F-E polymer film is regular without visible holes and big grains.

The surface of Oxad-6F-E thin film has appeared to be rather regular without any holes or big grains. That of the Oxad-6F-E thin films is not regular, big grains have appeared to coalesce into bigger continuous area.

3.2. IR measurements

IR absorption spectra covering $450-4050$ cm^{-1} wave number range performed on Oxad-6F-D and Oxad-6F-E thin films are shown in Fig. 9 and Fig. 10 respectively.

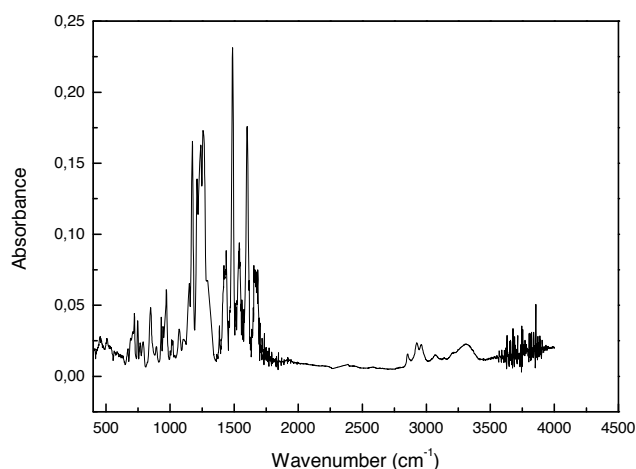


Fig. 9. IR absorption spectrum of Oxad-6F-D thin film deposited onto KBr pastille

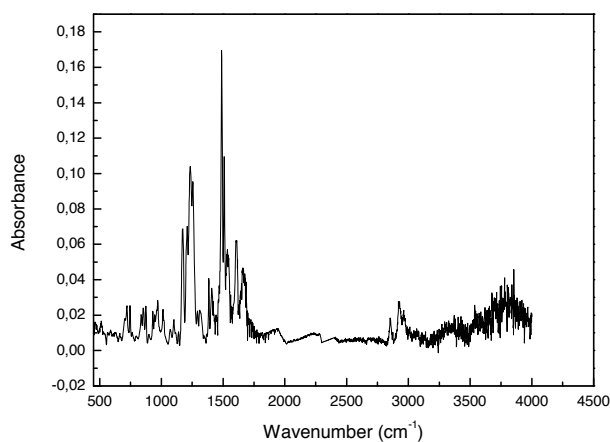


Fig. 10. IR absorption spectrum of Oxad-6F-E thin film deposited onto KBr pastille

It is clearly seen that the strongest peaks are seen at about 1173, 1256, 1488 and 1601 cm^{-1} wave number. Lower intensity peaks are seen at about 721, 848, 970, 1292 and 1664 cm^{-1} .

IR spectra taken on Oxad-6F-E thin films are shown in Fig. 10. The strongest peaks are visible at 1234, 1488, 1610 and 1669 cm^{-1} . The peaks of lower strength are at about 745, 910, 1013 and 2919 cm^{-1} .

3.3. UV-Vis measurements

UV-V is absorption spectra versus wavelength taken on Oxad-6F-D and Oxad-6F-E polyoxadiazoles thin films are shown in Figs 11-16. In each figure, there are shown three absorption spectra taken on thin films deposited from THF solutions of three different concentrations. The solution concentrations are visible on every graph.

Thin films of Oxad-6F-D and Oxad-6F-E deposited with spinning rate $V=3000$ rpm are shown in Fig. 11 and Fig. 12, respectively.

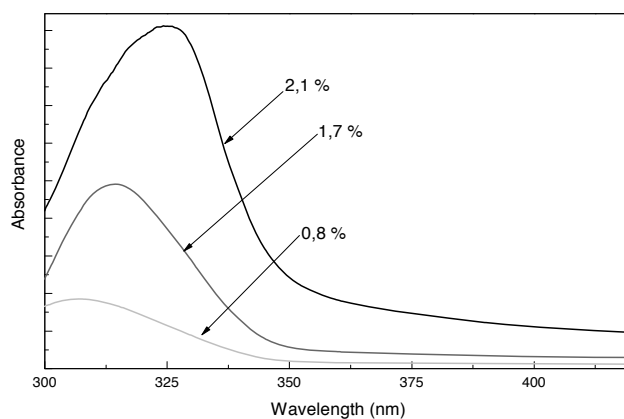


Fig. 11. Absorption spectra of Oxad-6F-D thin films deposited with spinning rate $V=3000$ rpm

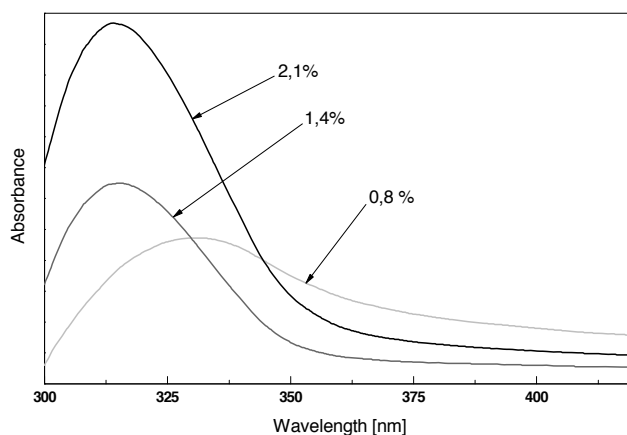


Fig. 12. Absorption spectra of Oxad-6F-E thin films deposited with spinning rate $V=3000$ rpm

It is seen in Fig. 11 that the absorption intensity increases as the solution concentration is on the increase. Absorption maxima of bands are at about 307, 314 and 325 nm for the solution concentration C equal to 0.8, 1.4 and 2.1%, respectively.

Similarly, in Fig. 12, the absorption intensity is seen to increase as the solution concentration is on the increase. The absorption maxima are seen at about 331, 315 and 331 nm for the solution concentration equal to 0.8, 1.4 and 2.1%, respectively.

UV-Vis absorption spectra taken on Oxad-6F-D thin films prepared with the spinning rates equal to 400 rpm are shown in Fig. 13. Absorption maxima are seen at about 307, 316 and 317 nm for the solution concentrations equal to 0.88, 1.70 and 2.1%, respectively.

UV-Vis absorption spectra of Oxad-6F-E thin films deposited with spinning rate $V=4000$ rpm, given in Fig. 14, the absorbance strength taken on the film deposited from 1.4% solution to be higher than the one in case of 2.1% solution.

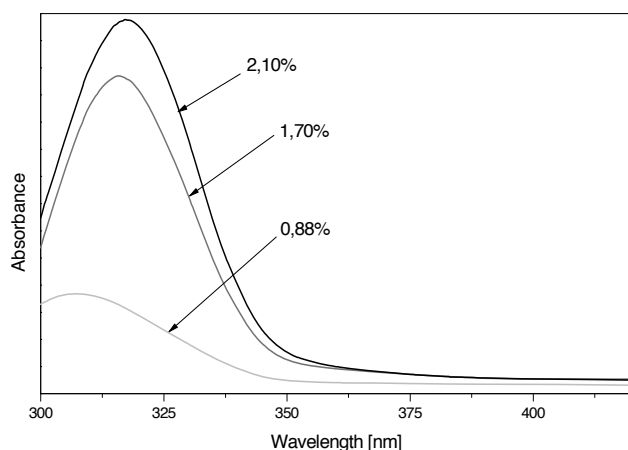


Fig. 13. Absorption spectra of Oxad-6F-D films deposited with spinning rate $V=4000$ rpm

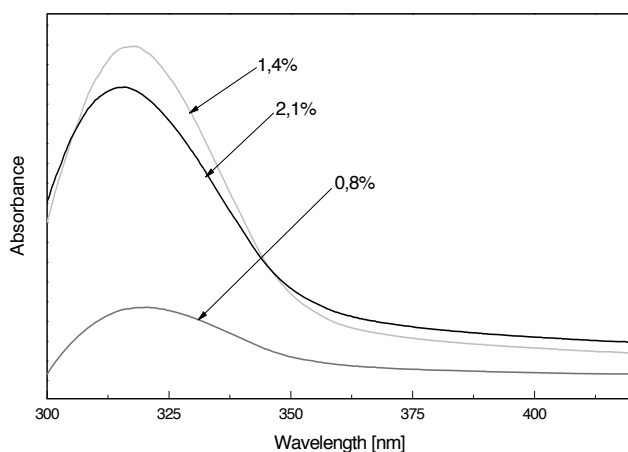


Fig. 14. Absorption spectra of Oxad-6F-E films deposited with spinning rate $V=4000$ rpm

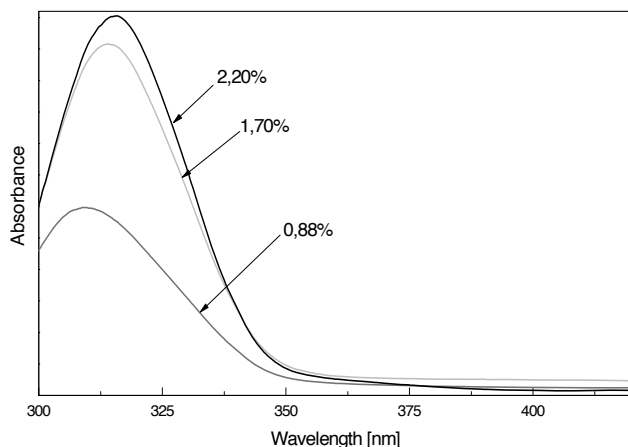


Fig. 15. Absorption spectra of Oxad-6F-D films deposited with spinning rate $V=5000$ rpm

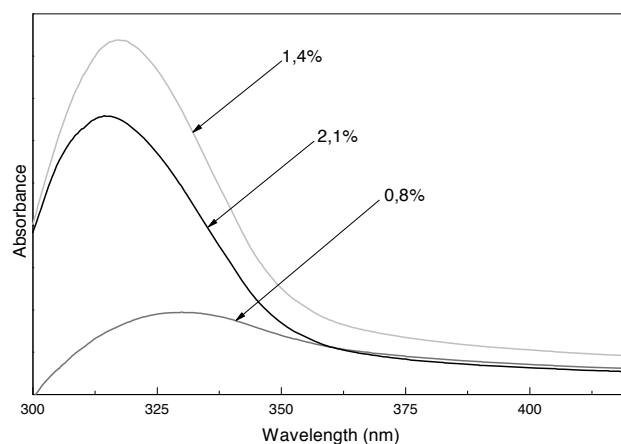


Fig. 16. Absorption spectra of Oxad-6F-E films deposited with spinning rate $V=5000$ rpm

The absorption maxima are seen at about 319, 315 and 317 nm for solution concentrations 0.8, 1.4 and 2.1%, respectively.

The absorption spectra recorded on Oxad-6F-D and Oxad-6F-E thin films deposited with the spinning rate $V=5000$ rpm are shown in Fig. 15 and Fig. 16.

The absorbance maxima are seen at about 319 nm for 1.4 and 2.2% solutions and at about 310 nm for 0.8% solution.

The absorption maxima in the spectra of Oxad-6F-E films are at about 319 nm for 1.4 and 2.2% solutions and at 329 nm for 0.8% solution.

4. Discussion

The spectra of Oxad-6F-D and Oxad-6F-E thin films covering $650-1800$ cm^{-1} wavenumber range were put onto one graph are shown in Fig. 17.

The peaks at 721 , 749 , 766 , 789 , 834 , 852 and 875 cm^{-1} are attributed to ring out-of-plane deformation vibrations carbon. The features peaking at about 930 , 970 , 1070 can be attributed to ring-in-plane deformation CCH vibrations. Peaks at about 1100 and 1173 cm^{-1} can be attributed to ring-in-plane CCH bending vibrations as well as to C-O vibrations connected with vibrations of ether linkages. Features seen within $1200-1250$ cm^{-1} are expected to be due to C-O-C ether linkages and amid group vibrations in the polymer backbone. In this area one may expect band resulting from C-F stretching vibrations. Strong peaks corresponding to CF_3 group vibrations and to -C-O-C- vibrations are in range $1200 - 1280$ cm^{-1} [16-17]. The strongest peaks at about 1488 , 1510 and 1540 cm^{-1} are attributed to aromatic phenyl ring vibrations. Higher intensity of 1540 cm^{-1} peak in the spectrum of Oxad-6F-D is attributed to meta-substituted benzene rings in its backbone. One may expect that some contribution to 1540 cm^{-1} band comes from amid group in the backbone. The peak seen at about 1601 cm^{-1} is expected to be due to stretching vibrations benzene rings. The peaks in range $1650-1700$ cm^{-1} are attributed to -C=C- or -C=N- double bond vibrations.

UV-Vis absorption spectra taken on Oxad-6F-D and Oxad-6F-E thin films, normalized to maximum of absorption bands are shown in Figs. 18-19.

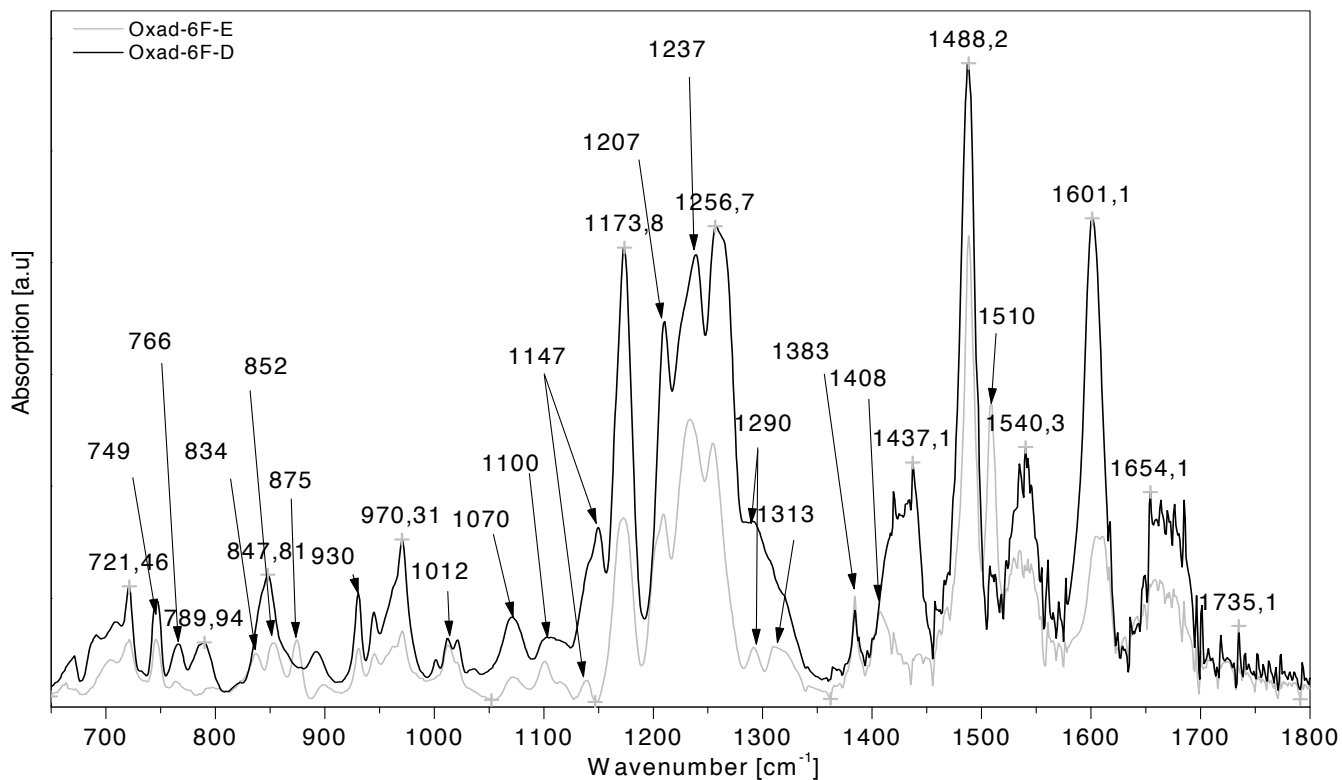


Fig. 17. IR spectrum of Oxad-6F-D and Oxad-6F-E thin polymer films in range 650-1800 cm^{-1}

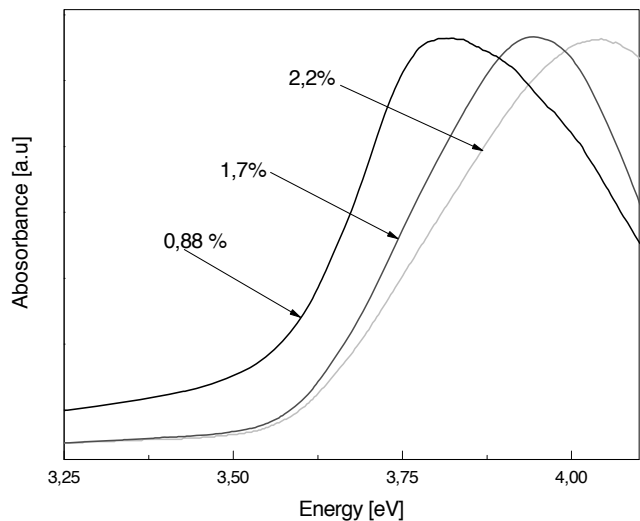


Fig. 18. Normalised UV-Vis absorption spectra of Oxad-6F-D thin films, deposited with the same spinning rate 3000 rpm and with three different concentrations

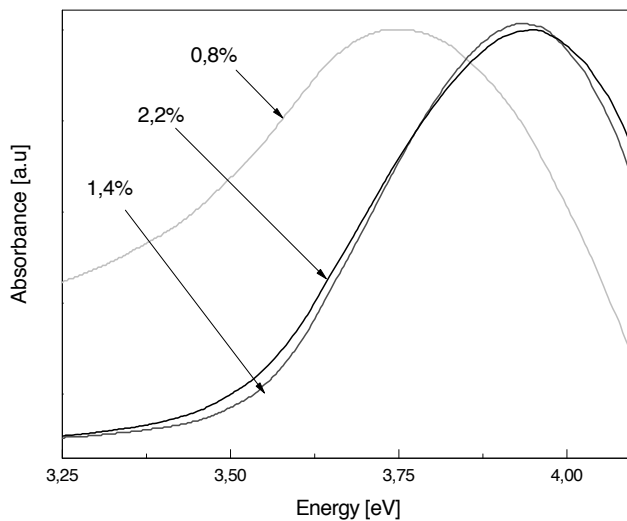


Fig. 19. UV-Vis absorption spectra of Oxad-6F-E thin films, normalised by the same spinning rate 3000 rpm and for three concentrations

Values of maxima of absorption bands are shown in Table 2. One can see, that maxima are shifted into higher energy with increase of concentration. However the difference between placement of individual bands is not too high. It is clearly seen that absorption intensity is increasing with the solution concentration on the increase, Fig. 11. This is attributed to shorter distances between polymer chains in thin films prepared from 1.7 and 2.0 % solution concentrations. Then, stronger interactions between polymer chains can be expected. The same displacement of absorption band were observed in case of Oxad 6F-E, however one can see, that changes of UV-Vis spectrum are more regular in case of Oxad-6F-D.

Table 2.
Oxad-6F-D and Oxad-6F-E absorption maxima

Oxad-6F-D		Oxad-6F-E	
C[%]	E [eV]	C[%]	E [eV]
0.8	3.81	0.8	3.74
1.7	3.94	1.4	3.93
2.2	4.04	2.2	3.95

The maximum of absorption band of Oxad-6F-D deposited from 0.8 % THF-polymer solution is placed at about 3.81 eV and absorption band of Oxad-6F-E deposited from the same concentration is at about 3.74 eV. The -1,-3 meta position of phenylene ring in Oxad-6F-D polymer chain caused conformation of polymer chain more complex than it is the case in the Oxad-6F-E thin film.

The highest rotation of the backbone cause, that Oxad-6F-D is more amorphous than Oxad-6F-E.

The AFM sensor and topographic images revealed irregular surface of polymer films. The images were taken on thin films deposited onto quartz substrates. To characterise roughness of polymer surface RMS and Ra [19] coefficients were determined with AFM software.

Ra is arithmetic mean of deviations in height from the profile mean value. Ra is defined as:

$$R_a = (1/N) \sum |Z_i - Z| \quad (1)$$

where: Z is sum of all height values Z_i divided by the N, which is number of data points.

The average RMS[18] and Ra coefficients are shown in Table 3.

Table 3.
RMS and Ra coefficients of Oxad-6F-D and Oxad-6F-E

Oxad-6F-D		Oxad-6F-E	
RMS [nm]	66	RMS [nm]	152
Ra [nm]	55	Ra [nm]	487

The RMS coefficient of Oxad-6F-E morphology and is equal to 152 nm and is higher than RMS of Oxad-6F-D which is equal to 66 nm. It is seen in AFM images that surface of both polymers looks similar. The morphology of polymer thin films is usually granular. The surface of Oxad-6F-D and Oxad-6F-E is ungranular - the grains are connected in bigger areas and diameter of connected grains is different.

5. Conclusions

The polyoxadiazole thin films were prepared with different technological conditions. The spinning rate V and solution concentration C were changed.

One can see, that both of technological parameters influenced UV-Vis absorption spectra. The absorption band intensity was increasing with solution concentration. Additionally the maxima of these bands were displaced towards higher photon energy with concentration.

In case of Oxad -6F-E the absorbance intensity of thin film prepared with 2,1% solution is lower than that of film prepared with 1.7 % solution.

The peaks seen in IR spectrum, in range 1205 -1295 cm^{-1} are attributed to strength vibration of CF_3 groups. The peak, which is seen at about 1601 cm^{-1} in IR spectrum of Oxad 6F-D and at about 1609 cm^{-1} in Oxad 6F-E spectrum is attributed to aromatic benzene ring vibrations. The observed differences on frequency values in IR spectra recorded on Oxad 6F-D and Oxad 6F-E are attributed to various substitution of phenylene ring in polymer chain.

AFM topographic images reveal granular morphology of Oxad -6F D and Oxad 6F-E. The surface of Oxad-6F-E film, prepared from 2.2% solution is smoother than surface of Oxad-6F-D film prepared from the same concentration of solution.

Acknowledgements

This paper has been done within the frame of the Project of Polish Ministry of Science Education and Education No N N507 4131 33 in frame of cooperation with Institute of Macromolecular Chemistry Romania Academy of Sciences in Iasi.

References

- [1] B. Schulz, Y. Kaminorz, L. Brehmer, New Aromatic Poly(1,3,4-oxadiazole)s for Light Emitting Diodes, *Synthetic Metals* 84 (1997) 449-450.
- [2] B. Schultz, L. Brehmer, B. Dietzel, Th. Zetzsche, Preparation and characterization of ordered thin film based on aromatic poly(1,3,4-oxadiazole)s, *Reactive and Functional Polymers* 30 (1996) 353-360.
- [3] E. Hamciuc, M. Bruma, T. Köpnick, Y. Kaminorz, B. Schulz, Synthesis and study of new silicon-containing polyoxadiazoles, *Polymer* 42 (2001) 1809-1815.
- [4] M. Bruma, T. Köpnick, Silicon-containing polyoxadiazoles-synthesis and perspectives, *Advances in Colloid and Interface Science* 116 (2005) 277-290.
- [5] S. Vetter, S.P. Nunes, Synthesis and characterizations of new sulfonated poly(arylene ether 1,3,4-oxadiazole)s, *Reactive and Functional Polymers* 61 (2004) 171-182.
- [6] D. Gomes, R. Marshall, S.P. Nunes, M. Wark, Development of polyoxadiazole nanocomposites for high temperature polymer electrolyte membrane fuel cells, *Journal of Membrane Science* 322 (2008) 406-415.
- [7] X.Y. Shang, D. Shu, S.J. Wang, M. Xiao, Y.Z. Meng, Fluorene-containing sulfonated poly(arylene ether 1,3,4-oxadiazole) as

- proton-exchange membrane for PEM fuel cell application, *Journal of Membrane Science* 291 (2007) 140-147.
- [8] D. Gomes, S.P. Nunes, Fluorinated polyoxadiazole for high-temperature polymer electrolyte membrane fuel cells, *Journal of Membrane Science* 321 (2008) 114-122.
- [9] M.S. Weaver, D.D.C. Bradley, Organic electroluminescence devices fabricated with chemical vapour deposited polyazomethine films, *Synthetic Metals* 83 (1996) 61-66.
- [10] L.A. Dobrzański, Engineering materials and materials design. Fundamentals of materials science and physical metallurgy, WNT, Warsaw, 2006 (in Polish).
- [11] B. Hajduk, J. Weszka, J. Jurusik, Influence of LCVD technological parameters on properties of polyazomethine thin films, *Journal of Achievements in Materials and Manufacturing Engineering* 36/1 (2009) 41-48.
- [12] B. Hajduk, J. Weszka, B. Jarząbek, J. Jurusik, M. Domański, Physical properties of polyazomethine thin films doped with iodine, *Journal of Achievements in Materials and Manufacturing Engineering* 24/2 (2007) 67-70.
- [13] J. Weszka, L.A. Dobrzański, P. Jarka, J. Jurusik, B. Hajduk, M. Bruma, J. Konieczny, D. Mańkowski, Studying of spin-coated oxad-Si properties, *Journal of Achievements in Materials and Manufacturing Engineering* 37/2 (2009) 505-511.
- [14] F. Taylor, Spin coating: An Overview, *Metal Finishing* 99/1 (2001) 16-21.
- [15] M. Deepa, T.K. Saxena, D.P. Singh, K.N. Sood, S.A. Agnihotry, Spin coated versus dip coated electrochromic tungsten oxide films: Structure, morphology, optical and electrochemical properties, *Electrochimica Acta* 51 (2006) 1974-1989.
- [16] B. Hajduk, J. Weszka, V. Cozan, B. Kaczmarczyk, B. Jarząbek, M. Domański, Optical properties of polyazomethine with oxygen atom in the backbone, *Archives of Materials Science and Engineering* 32/2 (2008) 85-88.
- [17] L. Marin, V. Cozan, M. Bruma, V.C. Grigoras, Synthesis and thermal behaviour of new poly(azomethine-ether), *European Polymer Journal* 42 (2006) 1173-1182.
- [18] F. Queirolo, M. Alessandri, A. Sassela, Influence of roughness and grain dimension on the optical functions of polycrystalline silicon films, *Thin Solid Films* 313-314 (1998) 243-247.
- [19] F.H. Pollak, B. Dorfman. Atomic force microscopy study of diamond-like atomic-scale composite films., *Thin Solid Films* 292 (1997) 173-178.